

## Driver behavior assessment based on the G-G diagram in the DVE system

Oussama Derbel and René Jr. Landry

*University of Québec, École de technologie supérieure,  
Montreal, Canada*

*e-mail: first-name.last-name@lassena.etsmtl.ca*

**Abstract:** This paper proposes a driving risk model based on the information given from the Driver-Vehicle-Environment (DVE) entities. It develops a two-level strategy to evaluate the driving risk. The first level aims to assess the risk locally in each entity and the second one concludes the global risk. The advantage of this approach is the simultaneous consideration of the parameters related to the DVE system regardless of information type (dynamic and static). It uses the Dempster-Shafer Theory (DST) for information fusion at each level. The approach uses Fuzzy Theory (FT) to design Basic Probability Assignment (BPA) functions, which is the significant part of the belief theory. The drivers' information for the driver risk evaluation the age and gender. Two parameters in the Vehicle entity are used in the cases of lane keeping and a left/right turn scenarios with utilizing two different developed Fuzzy Inference Systems (FIS). The first system uses an Euclidean acceleration-norm and the velocity of the vehicle; while, the second one, uses lateral/longitudinal acceleration based on G-G diagram and a proposed risk indicator.

The results of different scenarios validate the developed risk models using the sixth version of the Proportional Conflict Redistribution (PCR6) combination algorithm.

© 2016, IFAC (International Federation of Automatic Control) Hosting by Elsevier Ltd. All rights reserved.

*Keywords:* Fuzzy theory, risk assessment, G-G diagram, belief theory, Pay How You Drive, Pay Where You Drive

### 1. INTRODUCTION

Nowadays, inappropriate speed and acceleration are the major causes of drivers death in road accidents. According to Road Safety Canada Consulting (2011), 27% of casualties in 2011 are caused by speeding where 81% of them occur in highways. In addition, 30% of accidents take place at intersections according to Rocha et al. (2013). This leads to take into account not only the vehicle parameter's but also the environment aspects such as where you drive and as you drive. For example, the night driving is considered riskier than the day driving, according to the accident number, due mainly to the visibility.

In the last two decades, there are numerous research works that focus on the risk assessment in some particular driving situations such as lane keeping and braking. There are different autonomous vehicle-follower control systems such as ACC with co-operative vehicle-follower control was designed to reduce the rear-end crashes by adjusting the vehicle speed and the inter-distance with the follower vehicle. However, the acceptance of these systems by people depends on its intuitiveness, unobtrusiveness, and performances as discussed by Zhang et al. (2010). So, the design of such systems has to be based on a good framework that links the parameters related to the Driver, Vehicle and Environment to have a better risk estimation. Especially, the case of insurance application, the accuracy of the estimated risk is very important, because it is directly linked to the insurance charge according to the Pay How You Drive (PHYD) and Pay Where You Drive

(PWYD) models. Several works use the Hidden Markov Model (HMM) and the Gaussian Mixture Model (GMM) to estimate the driver skills as done by Meng et al. (2006) and Angkititrakul et al. (2011), respectively. However, these references were only concentrated on the vehicle parameters to assess the driving behavior and it is more judicious to consider the Driver and Environment entities.

This paper deals with the risk estimation based on the parameters of the DVE system using the Dempster-Shafer Theory (DST) and the sixth version of the Proportional Conflict Redistribution (PCR6) methods of Belief theory in the case of insurance applications. The developed risk models are designed to assess the driving risk in the case of lane keeping situation as well as the turning scenario using the G-G diagram. This latter was used in the literature to define the driving safety area based on the longitudinal and lateral accelerations. Based on this diagram a risk indicator is developed and integrated in a Fuzzy Inference System (FIS). Two developed FIS are used in the Vehicle entity to compute the driving risk level.

After the presentation of the problematic and our methodology to assess the driving risk in Section 2, Section 3 introduces the DST used for risk information fusion. Section 4, develops the risk models for each entity of the DVE system. Before the conclusion in Section 6, Section 5 presents the results of the proposed scenarios used to validate the proposed risk models.

## 2. PROBLEM STATEMENT AND METHODOLOGY

The evaluation of the driver safety remains a complex task due to the heterogeneity of the parameters in terms of time variation (e.g. driver age and vehicle velocity). Moreover, vehicle's parameters are measured using low-cost sensors, and therefore are noisy. The noise affects the driver safety indicators accuracy and makes the risk assessment more difficult, especially in the case of insurance applications, where the driver is charged according to his driving behaviors (PWYD and PHYD).

To take into account the heterogeneity of the parameters, Figure 1 presents the adopted fusion architecture. In this one, the noise is spread from the vehicle sensors level to the global decision level using the Dempster-Shafer theory of evidence. This theory allows taking into account the noise of the parameters by computing the belief and plausibility parameters. The difference between these two parameters is the uncertainty of the output given the errors of the inputs. Figure 1 shows two fusion levels while the first one is designed to fuse locally the risk of each entity of the DVE system, and the second one computes the global driving risk.

In this paper, the risk in Driver entity depends on the driver age and gender. In fact, analysis of accident statistic reveals that the driver's gender is an important factor that affects the traffic safety as shown in Figure 4a. In this figure, male drivers are less involved in accidents than female drivers for all ages. Therefore, the risks related to the age and gender are fused to obtain the local risk related to the Driver entity.

In the Vehicle entity, the longitudinal and lateral accelerations as well as the acceleration norm and the velocity are taken into account. The lateral and the longitudinal acceleration are evaluated together by means of the G-G diagram (more explanation is given in Section 4.3). The diagram is divided into different zones that characterizes the driving behavior, especially in the case of a curved road (e.g., right/left turns). Since the vehicle parameters are noisy, the fuzzy logic theory is applied in our framework to ensure the fuzzy passage between the different zones of the G-G diagram. From the insurance point of view, the Vehicle safety level serves to evaluate the insurance policy based on the PHYD model. Here, as the Vehicle risk level gets more important as the driver is considered aggressive and the insurance charge gets important.

According to the accident statistical analysis done by Gilbert and Halsey-Watkins (2013), the driving place, the time of the day, and the day of the week are of great importance. Figure 2 presents the normalized risk level related to the time of driving during the day which is considered in this paper.

## 3. DEMPSTER-SHAFFER THEORY OF EVIDENCE

The Dempster-Shafer Theory (DST) has been developed by Dempster (1968) and later on by Shafer (1976). The DST theory is based on the definition of the frame of discriminant composed by all the possible sets (or hypotheses). Let  $\Theta$  be the set of the hypotheses defined as  $\Theta = \{\theta_1, \theta_2, \dots, \theta_p\}$ , where  $\theta_p$  is a possible solution. The relative referential subset  $2^\Theta$  (power set) is then defined as

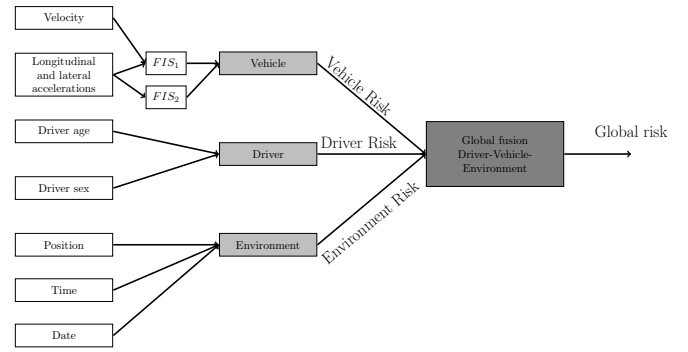


Fig. 1. Diagram for driving risk assessment

$$2^\Theta = \{\emptyset, \theta_1, \theta_2, \dots, \theta_p, \theta_1 \cup \theta_2, \dots, \Theta\}, \quad (1)$$

where  $\emptyset$  represents the conflict between sources and  $\Theta$  the ignorance (the union of all hypotheses). The belief in each hypothesis is represented by the mass, the Basic Belief Assignment (BBA) or the Basic Probability Assignment (BPA) defined as:

$$m : 2^\Theta \rightarrow [0, 1], \quad (2)$$

where  $\sum_{A \in 2^\Theta} m(A) = 1$  and  $m(\emptyset) = 0$ .

So, the DS structure is not a fuzzy measure since it is not required to have  $m(\Theta) = 1$ . Yager (1999) studied the difference between the Fuzzy and the DS theories and concludes that the DST allows representing an additional information to the fuzzy measure about the uncertainty in the parameter. In our framework, the algorithm developed by Boudraa et al. (2004) is used in the case of fuzzy measure.

The combination step is the third step of this theory. There are a variety of fusion algorithms in this part and the choice among them depends on the application. Daniel et al. (2013) suggest the use of the Proportional Conflict Redistribution (PCR) algorithm, which is developed by Smarandache and Dezert (2005), in the case of risk fusion. However, Daniel et al. (2013) used the fifth version of this algorithm that Martin and Osswald (2006) has demonstrated some drawbacks and propose the sixth version of the PCR given for  $N$  sources as follows:

$$m_{PCR6}(X) = \sum_{\theta_1 \cap \dots \cap \theta_p = X} \prod_{i=1}^N m_i(\theta_i) + \frac{\prod_{j=1}^{N-1} m_{\gamma_k(j)} \theta_{\gamma_k(j)}}{\sum_{k=1}^N m_k(X)^2 \sum_{\substack{\bigcap_{k=1}^{N-1} \theta_{\gamma_i(k)} \cap X = \emptyset \\ \theta_{\gamma_i(1)}, \dots, \theta_{\gamma_i(N-1)} \in (2^\Theta)^{N-1}}} \frac{m_k(X) + \sum_{j=1}^{N-1} m_{\gamma_k(j)} \theta_{\gamma_k(j)}}{m_k(X)^2}} \quad (3)$$

where  $\gamma_k$  is given by:

$$\begin{cases} \gamma_k(j) = j & \text{if } j < k \\ \gamma_k(j) = j + 1 & \text{if } j \geq k \end{cases} \quad (4)$$

The decision step is used to assign the output masses over the reference subset given by (1). In this paper, the Belief function is used to decide the risk output. More information about the decision function can be found in the reference of Martin and Osswald (2006).

#### 4. DRIVER-VEHICLE-ENVIRONMENT RISK MODELS

##### 4.1 Environment risk model

The environmental parameters have to be taken into account to assess the driving risk. In this paper, we consider both the place and the time of driving (the month of the year, the day of the week, and the time of the day). The choice of these parameters is based on the fact that the driving place gives a subjective risk evaluation using the accident number. Here, no matter that this place is a highway or an intersection. In fact, the accident can be caused by the absence of the traffic lights and/or the visibility in the intersection.

Based on the statistical analysis of accident presented by Gilbert and Halsey-Watkins (2013), the hour of the day risk model is developed using the normalized accident rate. This model is presented in Figure 2. As expected, the traffic presents the higher risk level between 5 pm and 7 pm since it is the most congested period of the day. In addition, there is a pic of high risk change at 8 am corresponding to the rush hour.

Using Figure 2, the thresholds between the different sets of the driving risk levels have been fixed. By means of these thresholds, the Expert model based BPA is developed and presented in figure 3 using trapezoidal and triangular membership functions. This Figure shows that between 12 pm and 6 am, the Environment risk related to the driving time is Low. The risk from 8 am to 10 am is qualified by neither High Risk (HR) nor Medium Risk (MR) but a risk between MR and HR. The advantage of the smooth transition between the defined risk levels in the developed expert model-based BPA can be shown between 3 pm and 7 pm in Figure 3. Here, the risk is considered to be high before it switches to a risk between HR and MR between 7 pm and 8 pm.

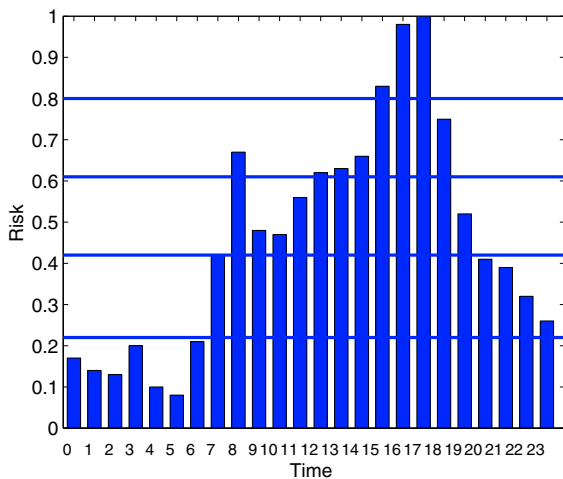


Fig. 2. Environment risk model based on the hour of driving in the day

##### 4.2 Driver risk model

In this paragraph, the Driver’s expert model-based BPA will be developed using the same method of paragraph 4.1.

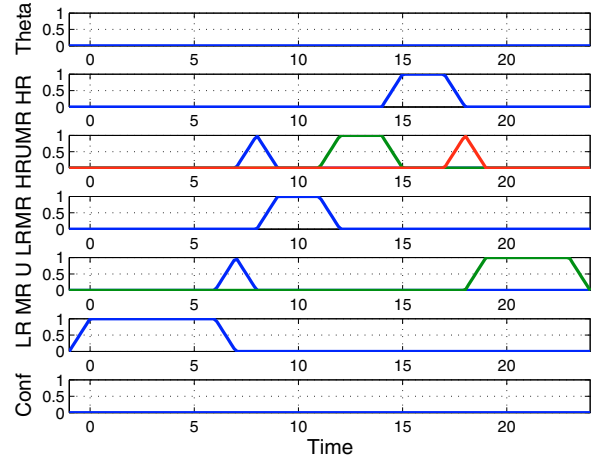


Fig. 3. Hours Basic Probability Assignment

In this paper, we will consider not only the age of the driver but also his sex. For this purpose, an expert model-based BPA is developed for each sex of driver.

*Age and gender risk models* Driver risk model depends on various parameters that can be classified as dynamic and static relative to the driving mission. The most important static parameters that affect the driver safety are the age and experience while the mood could be considered as variable. To study the impact of these parameters on driver safety, some researchers use the questionnaires and/or the physiological changes (e.g, facial muscles activities, eye tracking, heart activity,...). Moreover, statistical analysis of accident done by Rocha et al. (2013) reveals that the driver gender has an impact on the traffic safety. Figure 4a shows that men drivers are riskier than women according to the number of accident. At the same time, this figure shows that the women under 19 years old are less risky than those between 25 and 54 years old in terms of accident number. This is counter-intuitive since women under 19 years old are considered as teenagers and less experienced than those are elder. For this purpose, the accident rate has been normalized with respect to the demography of each age group presented in Figure 4a. Figure 4b presents the normalized risk with respect to the drivers gender and age. So, man are more risky than women and that the woman drivers under 19 years old are considered as more risky than the older ones. In the Figure 4b, we have defined the thresholds between the different risk levels ( $LR, LR \cup MR, MR, MR \cup HR, HR, HR \cup LR$ ) to develop subsequently the expert-model based BPA for each gender as done in the paragraph 4.1. This model will be used in the driving risk assessment in the Section 5.

##### 4.3 Vehicle risk model

Both the longitudinal and lateral accelerations are very important for the evaluation of the driver behavior, especially in the case of left/right turns scenarios. The longitudinal and lateral acceleration limits are highly related to the friction ellipse that defines the relationship between the tire and the road surface for different surface conditions. Vaiana et al. (2014) proposes a Driving Style Diagram (DSD) from the G-G diagram, which is presented in the

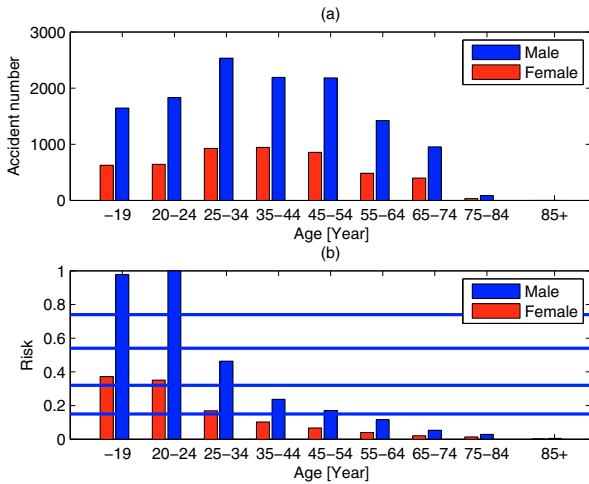


Fig. 4. (a) accident rate with respect to the driver age and gender [2006-2011] (b) Risk with respect to the driver age and gender [2006-2011]

Figure 5. This diagram assumes that the driving style is safe if the point with the coordinates of  $a_x$  (longitudinal acceleration) and  $a_y$  (lateral acceleration) is inside the diagram. Otherwise, the driving style is unsafe. The drawback of this approach is the binary evaluation of the driving behavior. In case of a driving mission, Vaiana et al. (2014) compute the percentage of point inside and outside the DSD to have an overview of the driving behavior. The limits of the safe area are fixed to  $2.5 \text{ m.s}^{-2}$  for the longitudinal and lateral acceleration in the case of left and right turns, and  $3 \text{ m.s}^{-2}$  is the limit of the longitudinal deceleration. The safe area limits were computed using an experimental dataset done by a single professional driver with different behaviors.

Our proposed method is twofold. The first one presents a new indicator to measure the driving style aggressiveness even inside the DSD by considering the distance from the origin of the diagram (point  $O$  in Figure 5) to the acceleration point (point  $I$  in Figure 5) and the distance from the origin to the intersection between the line passing from the acceleration point and the safe area limit of the DSD (point  $J$  in Figure 5). We define our indicator as

$$I_s = \left| \frac{OI}{OJ} \right|, \quad (5)$$

that is able to compute the aggressiveness degree of the driver even in case of safe driving situation.

The second level introduces a new area in the safety area of the DSD limited by the dashed lines as shown in Figure 5. These dashed lines represent the equation  $I_s = 0.5$ . The variability of the dashed line limits depends on the choice of the user to qualify the driving style, especially in the case of insurance applications. Nevertheless, as the acceleration gets important, the driving style is aggressive even in a safe area. When the acceleration is inside the area bounded by the dashed line, the driving style is considered as *good*. It is assumed *normal* when  $0.5 \leq I_s \leq 1$ . Otherwise, the driving style is considered *aggressive*. Since the limits in the G-G diagram for classifying good, normal and aggressive driving range are subject to change according to the environment model (e.g. date with respect to statistical density of weather/rain/road friction conditions)

and the vehicle parameters, the fuzzy approach is used. Using the defined G-G diagram in Figure 5, the DSD and the developed indicator, the fuzzy membership functions in Figure 6 are developed for the synthesis of the BPA by means of the Boudraa et al. (2004)'s method. This latter is used to compute the belief measurements from the fuzzy measurements given from the Figure 6. Then, the belief measurements related to the Vehicle together with those from the Environment and the Driver are used to evaluate the driver behavior in Section 5.

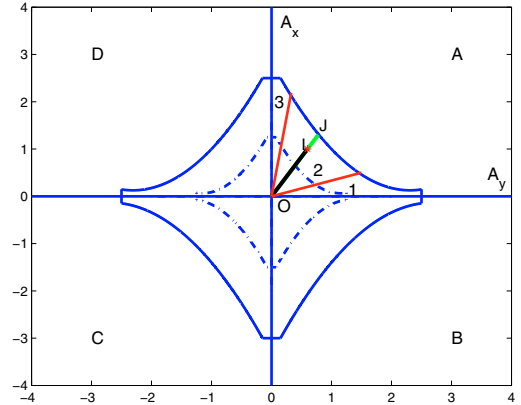


Fig. 5. The G-G diagram for Driver risk assessment

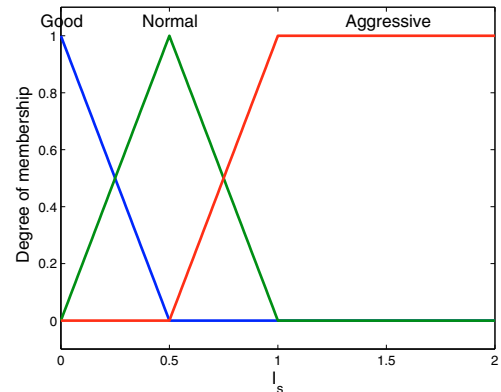


Fig. 6. Fuzzy membership functions of the developed safety indicator

## 5. EXPERIMENTAL RESULTS

### 5.1 Introduction

The goal of this section is to assess the driving risk in case of longitudinal driving and left/right turns scenarios through the developed risk models of the Driver-Vehicle-Environment system.

The risk is qualified as Low Risk (LR), Medium Risk (MR) or High Risk (HR) and the frame of discernment is defined by

$$\Theta = \{LR, MR, HR\}. \quad (6)$$

The relative referential subset is defined as:

$$2^\Theta = \{\emptyset, LR, LR \cup MR, MR, MR \cup HR, HR, HR \cup LR, \Theta\} \quad (7)$$

So, the goal is to evaluate the driving risk by generating masses over the propositions  $LR$ ,  $LR \cup MR$ ,  $MR$ ,  $MR \cup HR$  and  $HR$ . The test and validation results of the developed DVE risk models are made through static and dynamic data using *MATLAB* and the CarSim vehicle simulator. Two types of scenarios are presented in this section. The first type presents two cases of static data and the second one evaluates a group of static data gathered from a driving mission. Here, the macroscopic parameters (e.g. mean of the masses over the propositions and its standard deviation,...) are used to post-process the driving behavior.

## 5.2 Experimental tests and results

*Scenario # 1* The first static scenario considers a 45-year-old female driver who drives at 4 pm on Monday in July 2015 in the "Sud Ouest" district of Montreal (Canada). The velocity and the longitudinal and lateral accelerations of the vehicle are  $103.8 \text{ km.h}^{-1}$ , and  $-6 \text{ m.s}^{-2}$  and  $-0.55 \text{ m.s}^{-2}$ , respectively. This configuration is made to test the developed Driver entity risk models. At the global fusion level, this configuration involves a high conflict between the Driver entity, which assigns the total mass to the Low Risk ( $m(LR)=1$ ), and the Environment and Vehicle entities, where the total masses are assigned to the High Risk proposition at the local fusion level. The global fusion results remains coherent with the *a-priori* risk analysis using the PCR6 to combine the local risks. In fact, the PCR6 redistributes the risk over the propositions LR ( $m(LR)=0.3333$ ) and HR ( $m(HR)=0.6667$ ) and this reflects the driving situation since there is only the Vehicle entity exposed to the High Risk.

*Scenario # 2* This scenario takes the same parameters related to the Driver and the Environment entities of the first scenario. The main difference comes at the Vehicle entity. Here the Velocity of the vehicle is  $130 \text{ km.h}^{-1}$  and the longitudinal and lateral acceleration are equal to  $1 \text{ m.s}^{-2}$  and  $0 \text{ m.s}^{-2}$ , respectively. This configuration involves a high conflict at the Vehicle's local fusion level as well as the global fusion level. So, according to the acceleration-velocity FIS model, this latter assigns the total mass to the proposition HR ( $m(HR)=1$ ) since the speed limit in the road section is  $100 \text{ km.h}^{-1}$  whereas the vehicle speed is  $130 \text{ km.h}^{-1}$ . According to the G-G diagram and the developed fuzzy model, these latter distribute the masses over the propositions LR ( $m(LR)=0.08$ ), MR ( $m(LR)=0.32$ ), and the union of these two propositions  $LR \cup MR$  ( $m(LR \cup MR)=0.6$ ). The PCR6 redistributes the risk over the propositions LR ( $m(LR)=0.0059$ ), MR ( $m(MR)=0.0776$ ), HR ( $m(HR)=0.6915$ ), and the union of the two propositions  $LR \cup MR$  ( $m(LR \cup MR)=0.2250$ ).

The results of the global fusion reorganizes the distribution of the masses obtained at the local fusion level and assign it to the proposition LR ( $m(LR)=0.3984$ ) due to the masses obtained from the Driver entity at the local fusion level. The other masses are assigned to the propositions MR ( $m(MR)=0.0029$ ), HR ( $m(HR)=0.5760$ ) and the union of the two propositions  $LR \cup MR$  ( $m(LR \cup MR)=0.0228$ ).

*Scenario # 3* Figure 7 presents the parameters of the third test scenario. The goal is to give a global evaluation

of the driving behaviors at the end of the driving mission using the obtained masses in each simulation step. Here, the mean of the instantaneous masses over the referential subset given by equation (7) is used.

This scenario is performed using CarSim vehicle simulator and is divided into two parts. In the first one, the driver accelerates until reaching the speed limit of  $100 \text{ km.h}^{-1}$  at the time 8 s as shown in the Figure 7. From 8 s to 13 s, the driver starts making a zigzag trajectory at high speed with a high lateral deceleration that reaches  $-6 \text{ m.s}^{-2}$ . In this scenario, we assume that the driver is a 45-year-old woman and the test is performed on Monday, 19 January 2015 at 8 pm in the district "Outremont" in the city of Montreal. We consider that the speed limit in this straight two lanes road section is  $100 \text{ km.h}^{-1}$ .

The local fusion results related to each entity of the DVE system is presented in the Figure 8. The Driver entity's masses remain constant during the mission since the same driver has made the test ( $m(LR)=1$ ).

The Environment masses ( $m(LR)=0.25$ ,  $m(LR \cup MR)=0.5$ ,  $m(MR \cup HR)=0.25$ ) are constant since the driving place is not changed and the masses related to the driving time are constant from 8 pm to 11 pm as shown in Figure 3. In the same figure, the Vehicle entity's masses represent the mean of all the instantaneous masses computed in each simulation step.

The combination of the local risks of the Driver, the Vehicle, and the Environment involves a large conflict between these local risks. In fact, the risk of the Driver entity is Low ( $m(LR)=1$ ) while the Environment and Vehicle entities assigns masses over the proposition High Risk.

According to the PCR6, this algorithm allocates the large mean masses to the propositions LR ( $m(LR)=0.4630$ ), due to the low risk at the Driver and Environment entities, and HR ( $m(HR)=0.4070$ ) as a result of the risk related to the Environment and the Vehicle entities.

In the Vehicle entity, the mean masses obtained through the first FIS (see Figure 1) is divided between the propositions MR ( $m(MR)=0.0018$ ), HR ( $m(HR)=0.9982$ ), and the union of these two propositions  $MR \cup HR$  ( $m(MR \cup HR)=0.0291$ ). Here, the highest mass over the proposition HR is explained as follow: since the velocity limit during the simulation is fixed to  $100 \text{ km.h}^{-1}$  and the velocity of the driver varies from 0 to  $110 \text{ km.h}^{-1}$ , the time spent to reach the velocity limit is qualified by a high risk driving at the Vehicle entity. So, the driver spend the most amount of time with a velocity very lower than the velocity limit. During this period of time, the first FIS (see Figure 1), which is related to the speed and the acceleration norm, gives a risky situation while the second FIS, which is related to the G-G diagram, gives a safe situation since the longitudinal and lateral accelerations are within the safe area of the G-G diagram during the most portion of this period.

Once the velocity becomes close to the speed limit, the zigzag scenario begins and the norm of the vehicle accelerations exceeds the safe acceleration limit. Here the first FIS intervenes in the risk evaluation less than the second FIS. In fact, the evaluation of the risk is more based on the second FIS (see Figure 1) and the G-G diagram in case of the zigzag scenario. The masses ob-

tained from the second FIS are divided between the propositions LR ( $m(\text{LR})=0.0124$ ), MR ( $m(\text{MR})=0.0425$ ), HR ( $m(\text{HR})=0.8106$ ),  $\text{LR} \cup \text{MR}$  ( $m(\text{LR} \cup \text{MR})=0.0251$ ) and  $\text{MR} \cup \text{HR}$  ( $m(\text{MR} \cup \text{HR})=0.1094$ ). The obtained masses are explained as follow: when the vehicle is performing a zigzag, the lateral acceleration is varying from  $-6.4540 \text{ m.s}^{-2}$  to  $4.0158 \text{ m.s}^{-2}$ . So, when the acceleration is in the safe area of the G-G diagram, the masses of the second FIS will be divided between the other propositions excepts the HR one. Otherwise, the proposition HR will have the highest mass from the second FIS, which is obtained during the most portion of the time.

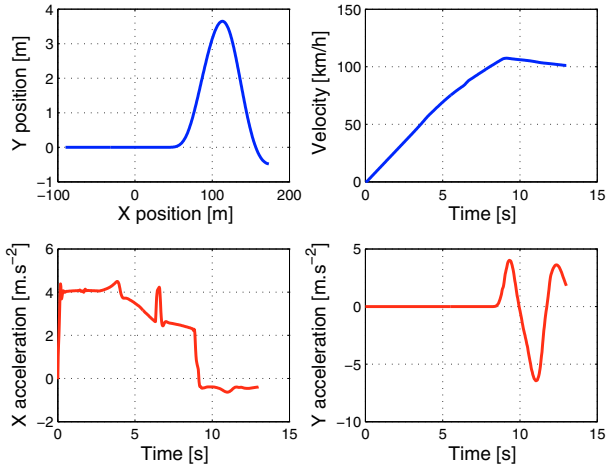


Fig. 7. ZigZag scenario at high speed

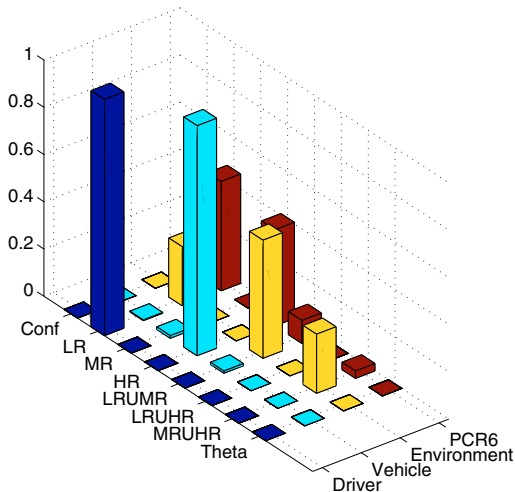


Fig. 8. Results of the scenario #3

## 6. CONCLUSIONS

This paper presented a driving behavior analysis based on the parameters related to the DVE entities in the case of longitudinal driving and ZigZag scenarios. The proposed approach takes into account the age and gender of the Driver, the place and time of driving in the Environment

entity and uses of G-G diagram in the Vehicle entity to develop an aggressiveness indicator inside the diagram and the related FIS model. The combination algorithm PCR6 has shown a good result in terms of conflict management between information sources.

Nevertheless, the presented work has to be more improved to by taking into account the driver's experience in the Vehicle entity and separating the risk coming from highways and residential areas in the Environment entity.

## 7. ACKNOWLEDGMENT

This research is part of the project entitled Vehicle Tracking and Accident Diagnostic System (VTADS). This research is partially supported by the Natural Sciences and Engineering Research Council of Canada (NSERC), École de technologie supérieure (ÉTS) within the LASSENA Laboratory in collaboration with two industrial partners namely iMetrik Global Inc. and Future Electronics.

## REFERENCES

- Angkititrakul, P., Miyajima, C., Takeda, K., 2011. Modeling and adaptation of stochastic driver-behavior model with application to car following. In: IEEE Intelligent Vehicles Symposium. pp. 814–819.
- Boudraa, A., Bentabet, A., Salzentein, F., Guillon, L., 2004. Dempster-shafer's basic probability assignment based on fuzzy membership functions. *Electronic letters on computer vision and image analysis* 4 (1), 1–9.
- Consulting, R. S. C., 2011. Road safety in canada. Tech. rep., Transport Canada.
- Daniel, J., Lauffenburger, J., Bernet, S., Basset, M., 2013. Driving risk assessment with belief functions. In: Intelligent vehicles symposium.
- Dempster, P., 1968. A generalisation of bayesian inference. *The royal statistical society B* 30 (2), 205–247.
- Gilbert, S., Halsey-Watkins, R., 2013. Cartes interactives des accidents routiers au québec.
- Martin, A., Osswald, C., 2006. A new generalization of the proportional conflict redistribution rule stable in terms of decision. *American research press* 2, 3–68.
- Meng, X., Lee, K., Xu, Y., 2006. Human driving behavior recognition based on hidden markov models. In: International Conference on Robotics and Biomimetics.
- Rocha, R., Guidoin, S., Déglise-Béland, G., 2013. Accident map of montreal.
- Shafer, A., 1976. A mathematical theory of evidence. The Princeton University Press.
- Smarandache, F., Dezert, J., 2005. Information fusion based on new proportional conflict redistribution rules. In: 7th International Conference on Information Fusion.
- Vaiana, R., Iuele, T., Astarita, V., Caruso, M., Tassitani, A., Zaffino, C., Giofrè, V., 2014. Driving behavior and traffic safety: An acceleration-based safety evaluation procedure for smartphones. *Modern Applied Science* 8 (1), 88–96.
- Yager, R., 1999. A class of fuzzy measures generated from a dempster-shafer belief structure. *International Journal of Intelligent Systems* 14 (1), 1239–1247.
- Zhang, Y., Lin, W., Chin, Y., Dec 2010. A pattern-recognition approach for driving skill characterization. *IEEE Transactions on Intelligent Transportation Systems* 11 (4), 905–916.